INTERNATIONAL JOURNAL OF CHEMICAL REACTOR ENGINEERING

*Volume* 4 2006 *Article* A9

# Modeling a Silicon CVD Spouted Bed Pilot Plant Reactor

Juliana Piña[*] Verónica Bucalá[†] Noemí Susana Schbib[‡]

Paul Ege[**] Hugo Ignacio de Lasa[††]

[*]Dep. of Chem. Eng., PLAPIQUI (U.N.S.- CONICET), Argentina, julianap@plapiqui.edu.ar

[†]Dep. of Chem. Eng., PLAPIQUI (U.N.S.- CONICET), Argentina, vbucala@plapiqui.edu.ar

[‡]Dep. of Chem. Eng., PLAPIQUI (U.N.S.- CONICET), Argentina, sschbib@plapiqui.edu.ar

[**]REC Silicon Inc., U.S.A, ege2606@rogers.com

[††]Chemical Reactor Engineering Centre, University of Western Ontario, Canada, hdelasa@eng.uwo.ca

ISSN 1542-6580

# Modeling a Silicon CVD Spouted Bed Pilot Plant Reactor

Juliana Piña, Verónica Bucalá, Noemí Susana Schbib, Paul Ege, and Hugo Ignacio de Lasa

## Abstract

This study reports a comprehensive multiphase gas-solid dynamic mathematical model that successfully describes the batch growth of silicon particles in a CVD submerged spouted bed reactor. This multiphase reactor model takes into account the hydrodynamics and interphase mass exchange between the different fluidized bed regions (spout or grid zone, bubbles and emulsion phase) and uses applicable kinetic rate models to describe both heterogeneous and homogeneous reactions. The model also incorporates a population balance equation representing particle growth and agglomeration.

The CVD submerged spouted bed reactor operation is simulated by means of a sequential modular procedure, which involves the solution of the reactor model and the population balance equation.

It is shown that the proposed CVD multiphase reactor model successfully simulates experimental data obtained from batch operation in a pilot scale reactor at REC Silicon Inc. The modeling of experiments obtained for different operating conditions allows correlating the scavenging factor as a function of the silane concentration for short- and long-term operations.

**KEYWORDS:** silicon CVD, spouted bed, granulation, modeling

# 1. INTRODUCTION

Over the past years, the solar photovoltaic industry (SPV) has experienced a strong expansion due to the inexhaustible and clean characteristics of the solar energy with respect to any conventional energy resource. At the present, the great demand of solar cells as modules to convert solar energy into electric power (which is expected to continue in the coming years) has exceeded the capacity of production of solar grade silicon (SG silicon) by approximately 50 % (Woditsch and Koch, 2002). As a result, the more expensive higher quality silicon for the manufacture of semiconductor devices is extensively used by the SPV industry. The standards for silicon employed in solar cell applications (SG silicon) are less stringent than those used in the electronic industry, with respect to impurities and morphology.

For a variety of reasons, the SG silicon has been typically obtained by thermal decomposition of gases containing silicon (silane, di-chlorosilane, tri-chlorosilane or tri-bromosilane) in hot rod (Siemens) reactors. This technique is expensive in both capital and operating costs being very desirable the adoption of an improved technology. In fact, the major impediments for the projected 25-30% annual growth rate in the SPV industry are the limited amount of supply and high price of the available SG silicon (Sarti et al., 2002).

Silicon chemical vapor deposition (CVD) by silane pyrolysis in fluidized beds constitutes an attractive alternative to produce ultra-pure silicon for the solar-cell industry. Compared with the Siemens-type reactor, the fluidized or submerged spouted bed reactor (FBR or SSBR) is a continuous process, offering considerably higher production rates and lower energy consumption. In this CVD-FBR process, which possesses the general advantages of fluidized bed technology (namely good contacting, thermal homogeneity, thorough mixing of particles, easy solids handling and low pressure drop), silane ($SiH_4$) is thermally decomposed into silicon and hydrogen and the silicon particles are produced by chemical vapor deposition on seed particles. Fluidized beds envisioned for this application contain a gas distribution grid. A specialized submerged spouted bed design (Lord et al., 1998) substitutes the dispersion grid with a submerged spout injector maintaining particles in a spouted circulation zone while keeping the upper zone where particles are fluidized in a bubbling regime. A tapered portion above the spout zone segregates particles by size. The silane and hydrogen gas mixture that holds the silicon seed particles in suspension can be introduced through the spout injector located at the bottom of the reactor. The bed is heated well above the silane decomposition temperature so silane decomposes and silicon is formed via two major pathways: a heterogeneous step where silicon deposits directly on existing seed particles by CVD and a homogeneous step where a new silicon solid phase is produced leading to formation of fines (Furusawa et al., 1988; Caussat et al., 1995a). The heterogeneous reaction is responsible for the major particle growth. In addition, fines can be agglomerated or scavenged by large particles as the gas/powder travel through the fluidized bed, also contributing to the particle growth. This specially designed submerged spouted bed incorporates all the process steps (seed formation, particle growth and particle separation) required to produce a well-defined granular product within a single unit.

The accurate modeling of the silicon CVD-FBR (i.e., hydrodynamics conditions, transport phenomena, homogeneous and heterogeneous reactions responsible for the silicon deposition and fines formation) constitutes one major development challenge for the reliable and successful scale-up from pilot to commercial units. In fact, one of the most important obstacles for the wide spread application of this process is the very expensive and time-consuming scale-up of the pyrolysis reactor (Tilg and Mleczko, 2000). While fluidized bed models are well established for processes including catalytic reactions, detailed models are still required for production of silicon by CVD in FBRs or SSBRs. Several mathematical descriptions, including the perfectly mixed (CSTR) reactor model, the classical and actualized Kunii and Levenspiel (1968; 1990) models and the bubble assemblage fluidized bed model (Kato and Wen, 1969), which accounted for the heterogeneous and homogeneous decomposition as well as CVD growth of seeds and scavenging of fines by large particles, have been presented in the literature to study the silane pyrolysis in FBRs (Lai et al., 1986; Li et al., 1989; Kojima et al., 1990; Caussat et al., 1995b; Tilg and Mleczko, 2000). Though various models have been proposed for bubbling fluidized beds, few have considered the importance of the grid zone (Kojima et al., 1990). As the heterogeneous and homogeneous silane decomposition rapidly proceeds at the operating temperature, the contribution of the grid zone to the bed performance may not be ignored. Moreover, most of the CVD-FBR published models are limited to monodispersed seeds that grow at the same rate up to an average final particle diameter (Lai et al., 1986, Hsu et al., 1987). This diameter; which depends on the rate of silicon deposition, the extent of scavenging and the average residence time of solids; influences the hydrodynamics of the bed as well as the mass transfer between phases. The use of average diameters to characterize

the particle size distribution is an approximation that should be removed to evaluate the particles growth rigorously (Tilg and Mleczko, 2000).

To evaluate the particle size distribution (PSD) as the particles grow, the fundamental balance equations of the CVD-FBR process (which provide the growth rate) have to be solved simultaneously with the population balance equation (PBE). The PBE constitutes an indispensable statement of continuity (an integro-partial-differential equation) for dealing with dispersed-phase systems, which describes the changes of PSDs due to particle growth, eventual agglomeration and attrition, seeds inflows or particles outflows by product sampling or extraction (Heinrich et al., 2002). The solution of the population balance equation requires special attention due to the discrete nature of particulate systems. Among the several numerical techniques proposed for solving PBEs, the discretization methods have been notably successful in a variety of applications since they have greatly reduced computational times (Ramkrishna, 2000). To avoid the numerical dissipation error caused by the discretization of the growth term the method of characteristics (MOC) was suggested (Kumar and Ramkrishna, 1997). This solution method consists of transforming the partial differential PBE into a system of ordinary differential equations that is then solved along the path line of the particles (characteristic curves). The particles are identified and located at the initial time and the population is tracked with a velocity equal to the growth rate (i.e., moving pivot technique). For granulation systems where agglomeration also takes place, Kumar and Ramkrishna (1996) proposed a numerical technique to properly reassign the agglomerated particles on the size grid, preserving the population mass and number.

A comprehensive mathematical semi-dynamic model that treats the batch growth of solids and the continuous steady-state behavior of the reactor gas phase is proposed in this work to describe the production of silicon by CVD in SSBRs. This multiphase reactor model takes into account the hydrodynamics and interphase mass exchange between the different regions (spout or grid zone, bubbles and emulsion phase) of the gas phase as well relevant kinetic expressions for both heterogeneous and homogeneous reactions. It also includes the population balance equation of growing particles, which is solved by the concept of combined MOC with the discretization method proposed by Kumar and Ramkrishna (1997), known as a very accurate and numerically stable technique for the calculation of the PSDs evolution over time in processes undergoing simultaneous particle growth and aggregation (Lee et al., 2001; Alexopoulos et al., 2005).

As it is shown in the present study this CVD multiphase reactor model, which carefully incorporates the contribution of various reacting phases, is proven to be successful to simulate the experimental data obtained from batch operation in a pilot scale reactor at REC Silicon Inc.

## 2. MATHEMATICAL MODEL

### 2.1. Process description

The submerged spouted bed reactor considered for silicon production by CVD is illustrated in Figure 1a (Lord et al., 1998). The bottom of this reactor is designed to promote deposition and particle growth as well as seed generation through spout attrition. The tapered region above the bottom is designed to promote segregation of larger particles to the bottom where they can be removed. The reservoir section serves as a granular filter capturing all the fines so they can deposit and contribute to particle growth as well.

During operation the bed is charged with silicon particles, fluidized with a preheated gas flow and heated to the reaction temperature. Then silane is increased until the desired silane concentration is achieved. Silane thermally decomposes to hydrogen and solid silicon. Most of the solid silicon is deposited heterogeneously on the particles in the SSBR, being the main mechanism of particle growth. The hydrogen and some entrained silicon fines (the fraction that is not captured in the bed by scavenging) leave the reactor. Granular silicon samples are withdrawn periodically from the reactor bottom to maintain the bed mass approximately constant. The particle size distribution (PSD) of each sample is determined by sieve analysis. At the end of the production run, all the particles are removed.

## 2.2. Submerged spouted bed reactor module

The multizone submerged spouted bed reactor model used to describe the silicon production by CVD from silane pyrolysis is schematized in Figure 1b (Errazu et al., 1979). Two regions in series are taken into account, an inlet spout zone followed by a developed fluid bed region. The gas flowing through the grid enters into the bed as a single spout. The spout exchanges gas with the surrounding dense emulsion. Two phases (bubble/emulsion) are considered for the fluid bed region. The gas from the spout flows through bubbles and mass is exchanged between bubbles and the adjacent dense phase.

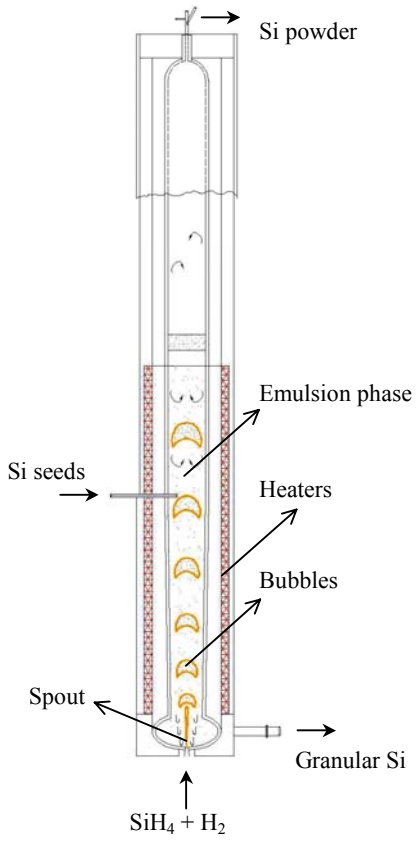


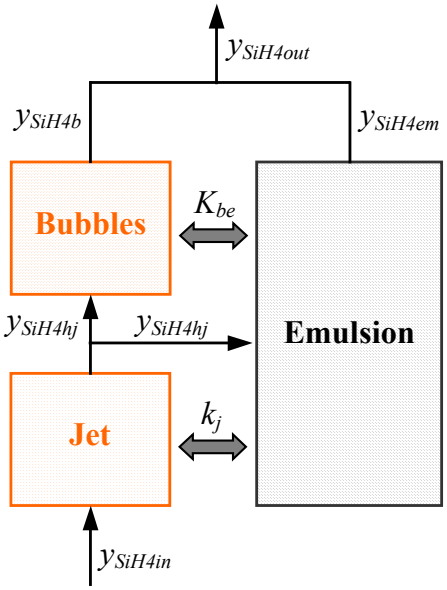


**Figure 1a.** Schematic representation of the spouted bed unit. **Figure 1b:** Scheme of the submerged spouted bed.

While silane pyrolysis in FBRs/SBBRs is governed by the overall reaction (1), the mechanism of decomposition is yet not completely understood (Caussat et al., 1995a).

$$SiH_4 \rightarrow Si + 2\,H_2 \qquad (1)$$

In this work, the silane pyrolysis is considered as a two-pathway reaction mechanism involving heterogeneous and homogeneous steps. The first order kinetics developed by Iya et al. (1982) and Hogness et al. (1936) are adopted to evaluate the heterogeneous and homogeneous reaction rates (equations 2 and 3), respectively (Lai et al., 1986).

$$r_{het} = k_{het} C_{SiH_4} \qquad (2)$$

$$r_{\hom} = k_{\hom} C_{SiH_4} \qquad (3)$$

The validity ranges, in terms of operating conditions, of these kinetic expressions are the following:

- For the heterogeneous reaction, temperatures between 873.15 and 1173.15 K and silane molar concentrations from 0.5 to 20% (Iya et al., 1982).
- For the homogeneous reaction, temperatures between 653.15 and 763.15 K and silane pressures from 11.3 to 74.2 kPa (Hogness et al., 1936).

The more recent kinetic model proposed by Furusawa et al. (1988) that takes into account the inhibiting effect of the reactants was also tested (equations 4 and 5).

$$r_{het} = \frac{k_{SO} C_{SiH_4}}{1 + K_{H_2} RTC_{H_2} + K_{SiH_4} RTC_{SiH_4}} \tag{4}$$

$$r_{hom} = \frac{k_{VO} C_{SiH_4}}{1 + K_V RTC_{H_2}} \tag{5}$$

For the conceptual multiphase reactor model illustrated in Figure 1b, the hypotheses summarized below are assumed.

a. Steady state for the gas phase and ideal gas behavior.
b. The spout has a uniform size and penetrates a distance $h_j$.
c. The gas in the spout is in plug flow.
d. The gas flow in the bubble phase corresponds to that in excess above the minimum fluidization conditions.
e. The bubbles have a uniform diameter.
f. The gas in the bubbles is perfectly mixed.
g. The bubbles rise in a plug flow.
h. The gas flow in the emulsion phase is at the minimum fluidization conditions.
i. The gas present in the emulsion phase is perfectly mixed.
j. The homogenous silane decomposition can take place in each of the three regions: spout, bubbles and emulsion.
k. The heterogeneous silicon deposition occurs in both spout and emulsion but is neglected in the bubbles in view of its low particle concentration (Hsu et al., 1984b; Li et al., 1989; Caussat et al., 1995b; Tilg and Mleczko, 2000).
l. The variations in the volumetric flow rate resulting from chemical conversion are not taken into account.

Under these assumptions, the mass balances for silane in the gas phase are given by the following equations:

***Gas Phase:***

Spout:

$$-\frac{dy_{SiH_4 j}}{dz} = \frac{k_j a_j A_{rj}}{F} \frac{(y_{SiH_4 j} - y_{SiH_4 em})}{M_{mix}} + \frac{r_{\hom j} \varepsilon_j A_{rj}}{F} + \frac{r_{hetj} S_{pj}}{h_j F} \tag{6}$$

Boundary condition: $z = 0$, $y_{SiH_4 j} = y_{\mathrm{SiH_4 in}}$ (7)

*Bubbles:*

$$-\frac{dy_{SiH_4 b}}{dt_R} = K_{be}(y_{SiH_4 b} - y_{SiH_4 em}) + \frac{r_{\hom b} N_{bubble} V_b U_b}{(F - F_{mf})(H - h_j)} \tag{8}$$

Boundary condition: $t_R = 0$ , $y_{SiH_4 b} = y_{SiH_4 h_j}$ (9)

*Emulsion Phase:*

$$y_{SiH_4 hj} F_{mf} - y_{SiH_4 em} F_{mf} + \frac{k_j a_j A_{rj}}{M_{mix}} \int_0^{h_j} \left(y_{SiH_4 j} - y_{SiH_4 em}\right) dz + \frac{K_{be} N_{bubble} V_b \rho_g U_b}{H - h_j} \int_0^{\frac{H-h_j}{U_b}} \left(y_{SiH_4 b} - y_{SiH_4 em}\right) dt_R = r_{hetem} S_{pem} + r_{\hom em} V_{gem} \tag{10}$$

The values and/or correlations employed for the estimation of the fluid dynamic, mass transfer and kinetic parameters are summarized in Table 1.

**Table 1.** Fluid dynamic, mass transfer and kinetic parameters.

| Parameter | Theoretical or empirical expression | Parameter | Theoretical or empirical expression |
|---|---|---|---|
| $k_{het}$ *(m/s)* | $2.79x10^6 \exp(-19{,}530/T)$ | $h_j$ $(m_j)$ | $2.23Q_{hole}^{0.35}$ |
| $k_{\hom}$ *(m/s)* | $2.x10^{13} \exp(-26{,}000/T)$ | $d_b$ $(m_b)$ | $0.667Q_{hole}^{0.375}$ |
| $k_{SO}$ *(m/s)* | $2.15x10^8 \exp(-23{,}033.4/T)$ | $U_b (m_r/s)$ | $U_0 - U_{mf} + 0.711\sqrt{(gd_b)}$ |
| $K_{H_2}$ *(1/kPa)* | 0.034 | $U_{mf}$ $(m_g^3/m_r^2 s)$ | 0.2 |
| $K_{SiH_4}$ *(1/kPa)* | $7.6x10^{-3} \exp(3{,}957.2/T)$ | $k_j$ *(kg/m$_j^2$s)* | $0.1\rho_g M_{mix}$ (Grace, 1986)<br>1.92 (Behie and Kehoe, 1973) |
| $k_{VO}$ *(1/s)* | $2.14x10^{13} \exp(-26617.7/T)$ | $K_{be}$ $(m_g^3/m_b^3 s)$ | $\frac{1}{\frac{1}{K_{bc}} + \frac{1}{K_{ce}}}$ |
| $K_V$ *(1/kPa)* | 0.5 | $K_{bc}$ $(m_g^3/m_b^3 s)$ | $\frac{4.5U_{mf}}{d_b} + \frac{5.85D_{mix}^{0.5} g^{0.25}}{d_b^{1.25}}$ |
| $\Delta P_d$ *(kPa)* | $\left(\frac{4Q_{hole}}{C_0 Y D_{hole}^2 \pi}\right)^2 \frac{(1-\lambda^4)}{2g_c} \rho_{gin} M_{mix}$ | $K_{ce}$ $(m_g^3/m_b^3 s)$ | $6.78\sqrt{\frac{\varepsilon_{mf} U_b D_{mix}}{d_b^3}}$ |
| $\Delta P_b$ *(kPa)* | $(1-\varepsilon_{mf}) \cdot (\rho_p - \rho_{gin} M_{mix}) g H_{mf}$ | $\varepsilon_{mf}$ $(m_g^3/m_{em}^3)$ | 0.42 |

The distributor pressure drop ($\Delta P_d$) is predicted from the practical working equation adopted by the ASME Research Committee on Fluid Meters for gas flow across nozzles (Miller, 1996). A nozzle type ASME long radius-nozzle is selected to estimate the value of the discharge coefficient through the correlations reported by Miller (1996). The bed pressure drop ($\Delta P_b$) is evaluated as suggested by Kunii and Levenspiel (1991). The spout penetration height and the bubble diameter are calculated using the formula derived by Basov et al. (1969). The bubble rise velocity is evaluated by means of the correlations given in Davidson and Harrison (1963).

The spout-emulsion mass transfer coefficients ($k_j$) reported by Behie and Kehoe (1973) and Grace (1986) are tested. For the experimental data available from REC Silicon Inc. and the mentioned spout-emulsion mass transfer coefficients, the kinetics reported by Furusawa (1988) does not predict well the granule/powder product ratio even when different scavenging factors are considered. For this reason and according to Lai's approach (Lai et al., 1986), the kinetics proposed by Iya et al. (1982) and Hogness et al. (1936) are adopted. Regarding the spout-emulsion mass transfer coefficient, the selection of the value reported by Behie and Kehoe (1973) over the one that results from the expression given by Grace (1986) was based on the tests. This $k_j$ value allowed to fit the experimental data of conversion and selectivity (granular/powder product ratio) at various operating conditions. The overall mass transfer coefficient between bubbles and emulsion ($K_{be}$) is estimated from the equations published by Kunii and Levenspiel (1991).

The heterogeneous CVD silicon deposition is assumed to take place in both the spout and emulsion, according to the fraction of total surface area of silicon particles available in each phase. The surface area of particles in the spout $S_{pj}$ is calculated from the spout void fraction $\varepsilon_j$, which is obtained by solution of the continuity equation (11) for particles moving at the cross sectional area of the bed in the spout zone. As it can be seen in the outline of the physical model considered to represent the submerged spout zone (Figure 2), its cross sectional area is divided in two regions, a spout in the center and the annulus around it. Particles in the annulus descend as in a moving bed and gradually enter into the center spout. The particles introduced in the spout initially have a null velocity, and soon begin to rise pneumatically in the spout by getting momentum from the ascending gas introduced through the nozzle.

$$v_{sa}\frac{\pi(D_R^2 - D_{hole}^2)}{4}\rho_p(1-\varepsilon_a) = v_{sj}\frac{\pi D_{hole}^2}{4}\rho_p(1-\varepsilon_j) \tag{11}$$

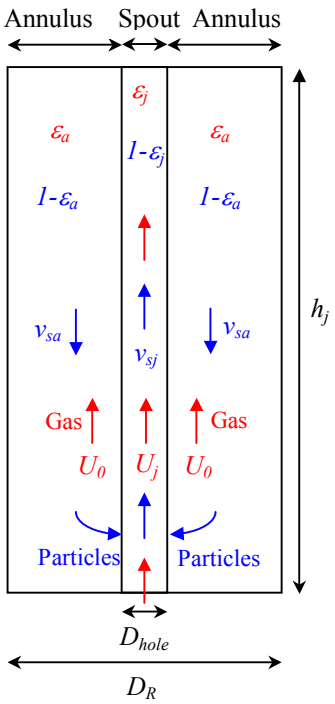


**Figure 2.** Schematic model of the submerged spout zone.

The upward particle velocity in the spout $v_{sj}$ is calculated by integration of equation (12) from the reactor inlet ($z_j$=0) to the spout penetration ($z_j$=$h_j$). This well-known equation represents the one-dimensional unsteady motion of one particle through a fluid due to gravitational, buoyant and drag forces. The drag coefficient $C_D$ is evaluated using the correlations reported by Haider and Levenspiel (1989) for particles with a given sphericity $\phi_s$.

$$W v_{sj} \frac{dv_{sj}}{dz_j} = gW - \frac{W}{\rho_p} \rho_g M_{mix} g - \frac{C_D v_{sj}^2 \rho_g M_{mix}}{2} \frac{\pi d_{p,mean}^2}{4} \tag{12}$$

Boundary condition: $z_j = 0$, $v_{sj} = 0$ (13)

Even though the energy balance in each of the three regions (spout, bubbles and emulsion) is not included in the presented SSBR mathematical model; different temperatures for the spout and fluidized bed (based on experimental data obtained in a pilot scale reactor at REC Silicon Inc.) were imposed.

## 2.3. Population balance equation module

The mathematical model presented for the submerged spouted bed module (Section 2.1.) is a valuable tool to represent the performance of the gas phase, but it cannot be used by itself to describe the behavior of the particle size distribution. To do this, a population balance equation (14) for a dynamic particulate system undergoing simultaneous particle growth and aggregation is included.

$$\frac{\partial n}{\partial t} + \frac{\partial (nG)}{\partial L} = B_A - D_A \tag{14}$$

Equation (14) relates, for a batch system, the accumulation of particles (in terms of the number density function $n$, i.e. particle number per unit size) (first term of the LHS) with the convective flux along the size (particle volume) axis $L$ (second term of the LHS) and the particle birth and death rates due to agglomeration (first and second terms of the RHS, respectively). $G$ is the volume growth rate.

By using the concept of the combined Method of Characteristics with the discretization techniques proposed by Kumar and Ramkrishna (1996) the general PBE with growth and aggregation (equation 14) can be expressed as the following ODE system:

$$\frac{\mathrm{d}N_i}{\mathrm{d}t} = \sum_{\substack{j,k \\ L_{i-1} \le L \le L_{i+1}}}^{i \ge j \ge k} (1 - \frac{1}{2}\delta_{kj}) \eta \beta_{kj} N_j N_k - N_i \sum_{k=1}^{M} \beta_{ik} N_k \tag{15}$$

$$\frac{\mathrm{d}d_{pi}}{\mathrm{d}t} = \frac{2}{\pi d_{pi}^2} G \frac{S_{pi}}{S_{pt}} = \frac{2}{\pi \sum_{i=1}^{M} d_{pi}^2} G \tag{16}$$

Boundary condition: $t = 0$, $d_{pi} = d_{pi,0}$ (17)

The above ODE system, which allows predicting the changes in the particle size distribution with time on stream, is subjected to the following assumptions:

a. The growth of solids follows a batch mode of operation.
b. The bed is perfectly mixed.
c. Particles are distributed among discrete size intervals characterized by a diameter $d_{pi}$ equal to the arithmetic mean of the corresponding $i^{th}$ size range.
d. The seeds are idealized spherical particles with a sphericity $\phi_s$.
e. The PSDs in the spout and emulsion phases are identical.
f. The total growth rate $G$ is distributed among the size intervals according to the fraction of total surface area of silicon particles inside the size range ($S_{pi}/S_{pt}$, see equation 16).
g. The particle size distributions of the withdrawn samples are representative of the bed PSDs, no segregation is considered.

The silicon particle growth is attributed to two simultaneous contributions: heterogeneous chemical vapor deposition in both spout and emulsion and scavenging of fines generated by homogeneous reaction in each of the three gas-phase regions (equation 18). The scavenging of fines is assumed to be proportional to the total amount of silicon powder produced, without distinguishing the scavenging efficiencies of each reactor phase.

$$G = \frac{M_{Si}}{\rho_p}\left[\left(r_{hetj} S_{pj} + r_{hetem} S_{pem}\right) + \alpha\left(r_{\hom j}\varepsilon_j A_{rj} h_j + r_{\hom b} N_{bubble} V_b + r_{\hom em} V_{gem}\right)\right] \tag{18}$$

The scavenging coefficient is within the $0 \le \alpha \le 1$ range, being its value dependent on whether none, some or all the powder is collected and incorporated by the large particles. The $\alpha$ parameter represents an average constant value of the scavenging factor along the batch time-on-stream.

For each class, the diameter growth rate (equation 16) is independent of the particle size but dependent on the total available surface area (i.e. all the particles diameters grow at given time with the same rate)

The factor $\eta$, proposed by Kumar and Ramkrishna (1996) to preserve the total number and mass when a new particle is formed by agglomeration, is given by equation (19).

$$\eta = \begin{cases} \dfrac{L_{i+1} - L}{L_{i+1} - L_i} & L_i \le L \le L_{i+1} \\ \dfrac{L - L_{i-1}}{L_i - L_{i-1}} & L_{i\text{-}1} \le L \le L_i \end{cases} \qquad L = L_j + L_k \tag{19}$$

where $L_j$ and $L_k$ denote a capturing particle size and a captured particle size in binary collisions, respectively. The agglomeration efficiencies or $\beta$ kernel factors involved in equation (15) were considered zero were considered zero for particle diameters larger than 500 μm (critical diameter for particles aggregation) and size-independent for smaller particles.

The SSBR-PBE model involves only two adjustable parameters, the scavenging and aggregation factors ($\alpha$ and $\beta$). Their values are determined by comparing model predictions with particle size distributions (more than 100 experimental data for each run) from solids batch operations in a pilot scale reactor at REC Silicon Inc.

## 2.4. Numerical solution

To deal with the dynamic particle growth that takes place in the silicon CVD submerged spouted bed reactor, the SSBR (gas-phase) and PBE (solid-phase) modules are combined according to the calculation scheme presented in Figure 3.

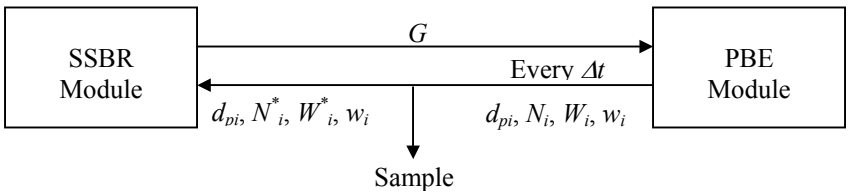


**Figure 3**. Scheme of the iterative calculation procedure used to simulate the batch silicon CVD-SSBR process.

The particle mass and size distribution, operating conditions and reactor geometry are the inputs for the SSBR module. The outputs of the SSBR module are the silane molar fraction in the spout (along the spout penetration), bubbles (as a function of the bubble residence time) and emulsion; which together with the PSD allow us to calculate, among others variables, the particle growth rate *G*. This *G* value and the particle size distribution constitute the inputs for the PBE module (dynamic model). The output of the PBE module is the particle size

distribution after a given time step $\Delta t$ (selected to minimize the CPU time without losing accuracy in the simulation results) much lower than the time interval between samples (removals extractions). At the beginning, the particle surface area available for growth is determined by the PSD of the seeds. As the CVD process progresses (i.e., at each $\Delta t$), the particle surface area existing for deposition is updated in the SSBR module by considering the PSD provided by the PBE. If product is removed, the particle number ($N_i$) and mass ($W_i$) for each size range ($d_{pi}$) at the moment of sampling are recalculated ($N^*_i$ and $W^*_i$), while the dimensionless mass distribution ($w_i$) remains unchanged. The system evolves in the described way up to the final operating time of the experimental run being simulated.

The described calculation procedure allows predicting the reactor performance, i.e. silane conversion rate, granule/powder product ratio, particle growth rate and the particle size distributions as a function of time on stream.

#### 2.4.1. Submerged spouted bed reactor module

To simulate the behavior of the gas phase, the set of algebraic and ordinary differential equations (6) to (13) must be solved simultaneously. By taking advantage of the structure of the SSBR model, a reasonably efficient iterative calculation procedure can be developed. The silane molar fraction in the emulsion phase ($y_{SiH4em}$) is common to all the mass balances (spout, bubbles and emulsion) and thus constitutes the natural iteration variable. First of all, the particle velocity $v_{sj}$ is determined by integrating the ordinary differential equation (12) through a Gear routine and the void fraction in the spout $\varepsilon_j$ is calculated from equation (11). Then the ordinary differential equations for the spout and bubble regions (6 to 9) are integrated by means of a Gear routine for an initial estimate of $y_{SiH4em}$. Once the silane molar fraction profiles in the spout and bubbles are obtained (as a function of the penetration and the bubble residence time, respectively), the integrals involved in the third and fourth terms of the LHS of equation (10) are evaluated through the Parabolic Rule (Simpson's Rule). After that, the non-linear algebraic equation (10) (silane mass balance in the dense phase) is solved using a Quasi Newton algorithm. The resulting new estimate of $y_{SiH4em}$ is utilized to start (reinitiate) a new iteration, until convergence is reached.

#### 2.4.2. Population balance equation module

The inputs for the PBE module are the particle size distribution and growth rate $G$. The integration of the differential equations (16) and (17) by means of a Gear routine enables to simulate the changes in the PSD due to growth and aggregation. The initial number of particles in each size interval $N_{i,0}$ is obtained from the initial bed weight $W_0$ and the initial seeds size distribution expressed in terms of mass fractions (i.e., $w_{i,0}$ vs. $d_{pi,0}$).

## 3. RESULTS AND DISCUSSION

In the present work, the results of the predictions of the CVD SSBR-PBE model are compared with experimental data obtained in a pilot unit (approximately of 15 $dm^3$) constituted by a lower spout section with a single central nozzle and an upper fluid bed section. Between these sections there is a gradual transition. An abrupt change of cross sections was assumed for modeling purposes. Operation was semi-batch and continuous modes for solids and gas-phase, respectively. The available experimental measurements, provided by REC Silicon Inc., are: operating conditions (pressure, temperature and flow rates), initial bed mass, sampling time, sample mass and PSD, and overall product split at the end of the run (granular product/silicon powder found in cyclone and filter).

To analyze the CVD-SSBR simulator performance, experiments with the following operating conditions were considered: $T_{in}$ = 473-673 K, $T_b$ = 873-1073 K, $P_{in}$ = 100-200 kPa, $y_{SiH4in}$ = 0-50 %, $t_f$ = 4-12 h, $U/U_{mf}$ = 5-6, $dp_{mean,0}$ = 800 μm. These values are within the operating ranges commonly reported (Hsu et al., 1987; Li et al., 1989; Lord et al., 1998; Tilg and Mleczko, 2000; Tejero-Ezpeleta et al., 2004).

For the selected operating conditions, the predicted silane conversion is almost complete for all the experiments, being this parameter almost independent of the adopted spout-emulsion and bubble-emulsion mass transfer coefficients. However, the calculated selectivity to granular silicon production by heterogeneous reaction and fines scavenging is sensitive to the mass exchange between phases, particularly in the spout-emulsion

interphase. The mass transfer coefficients affect the silane contact efficiency with Si-surface and hence the selectivity towards CVD, i.e. high mass transfer increases heterogeneous deposition.

The solution of equations (11) and (12) led to relatively high spout void fractions, being the particle surface areas available in the spout several orders of magnitude less than those in the emulsion. As a result, the model predicts low silane conversions in the spout due to heterogeneous reaction. The CVD-SSBR model including the spout may contribute to improving the grid region design in order to obtain large exchange coefficients and therefore good gas-solid contact to suppress the fines formation (Lai et al., 1986).

The scavenging factor was adjusted for all the experiments in order to correctly reproduce the evolution of the bed mass. As an example, Figure 4 shows for a base case the experimental and predicted dimensionless bed masses for two different values of the scavenging factors after stable operation was reached. As it can be seen, the bed mass is underestimated when null scavenging is assumed. However with a constant scavenging factor over time, the CVD-SSBR model tracks well the experimental data. The calculated $\alpha o$ value indicates that the solids capture a majority of the homogeneous production in the emulsion phase. This result is in good agreement with process observations, which suggest that significant amounts of powder material are scavenged and deposited on particles. The experimental evidence implies a relatively high bubble-emulsion powder mass transfer.

Since process experience indicates little agglomeration without fines ($d_p$ < 500 μm), the $\beta$ factors in the agglomeration terms of equation (15), which assign the probability of binary collisions, were considered zero for particle diameters larger than 500 μm (critical diameter for particles aggregation). For smaller particles, the kernel factors are assumed to be equal for all the particle classes. Agglomeration does not generate mass; therefore it does not affect the mass balance. However it influences the particle growth and size distributions. As only the smaller particles have probability to agglomerate, the total solid surface area changes over time due to particles aggregation are not significant. For this reason, the scavenging factor $\alpha$ and the agglomeration efficiency $\beta$ can be fitted independently. Once the $\alpha$ value was established, the $\beta$ factor was adjusted to fit the mean particle diameter along the duration of the experiment. Figure 5 presents the mean particle diameter as a function of time with and without agglomeration, for the experiment selected as the base case. The $\beta$ parameter allowed tracking satisfactorily the trend exhibited by $d_{pmean}$.

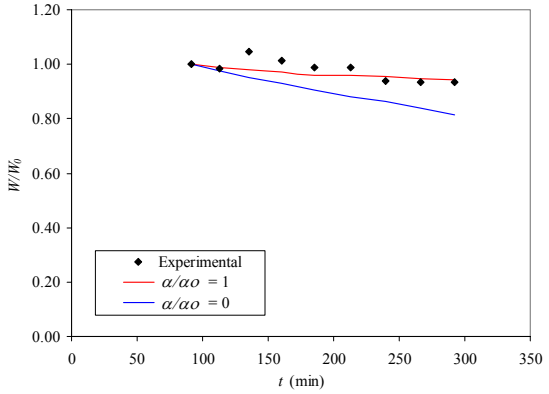


**Figure 4:** Experimental and predicted bed masses as function of time for the base case.

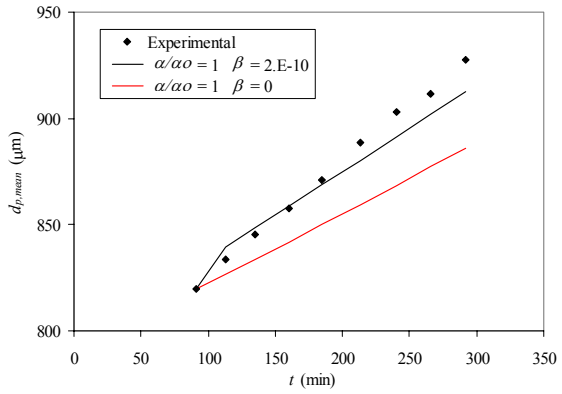


**Figure 5:** Experimental and predicted mean particle diameter as function of time for the base case.

The PSDs shown in Figure 6, for the base case at different times on stream, indicate that the particle size distributions are well predicted by the proposed SSBR-PBE model with just $\alpha$ and $\beta$ as adjustable parameters. Figure 6a also presents the initial PSD, as it can be seen the mass fraction of the smaller particles diminishes as a consequence of the simultaneous growth and agglomeration phenomena.

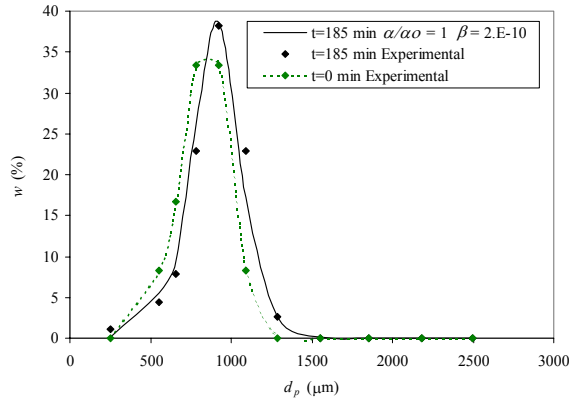


**Figure 6a:** Experimental and predicted PSD for the base case at $t$ =185 min.

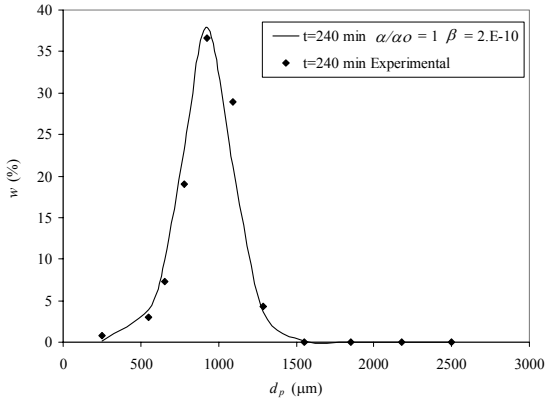


**Figure 6b:** Experimental and predicted PSD for the base case at $t$ =240 min.

Table 2 presents the operating conditions, granular production (*GP*), mean final particle diameter, average growth rate and the fitted model parameters ($\alpha$ and $\beta$) for five selected experiments. These data were chosen to analyze the influence of different operating variables on the CVD-SSBR performance, particularly on the granular production and scavenging efficiency. The experiment E1 was selected as the base case, while E2 to E5 were experiments characterized by almost the same operating variables as E1 with exception of one of them, which was varied in greater proportion to explore its effect on the process.

**Table 2:** Operating conditions, granular production, mean final particle diameter, average growth rate and fitted model parameters for experiments E1 to E5. The dimensionless variables are relative to the base case E1 (represented by subscript *o*).

| **Experiment** | **E1** | **E2** | **E3** | **E4** | **E5** |
|---|---|---|---|---|---|
| $T_j/To$ | 0.9 | 0.9 | 0.95 | 0.9 | 0.9 |
| $T_b/To$ | 1 | 1 | 1 | 0.9 | 1 |
| $F_{H2in}/Fo_{H2}$ | 1 | 1.8 | 1 | 1 | 1 |
| $F_{SiH4in}/Fo_{SiH4}$ | 1 | 1 | 1 | 1 | 1.25 |
| $y_{SiH4in}/yo$ | 1 | 0.61 | 0.97 | 0.96 | 1.21 |
| $GP^*/GPo$ | 1 | 0.67 | 0.99 | 0.96 | 1.01 |
| $d_{pmean,f}$ (μm) | 989 | 954 | 980 | 977 | 104 |
| $\alpha/\alpha o$ | 1 | 0.55 | 1.09 | 0.91 | 1.27 |
| $\beta$ | 2.E-10 | 1.5E-10 | 1.8E-10 | 4.E-10 | 3.E-11 |
| $G/Go$ | 1 | 0.71 | 1.06 | 0.80 | 1.20 |

* *GP* is defined as the amount of silane that produces granular silicon (by the heterogeneous reaction, the homogeneous reaction combined with the scavenging phenomenon and the agglomeration process) with respect to the total quantity of silane that reacts.

For E2 the disturbance variable was the hydrogen flow rate, which was increased in about 80% with respect to the nominal one (E1). Higher hydrogen flow rates for a constant value of the silane flow rate led to an important reduction of the inlet silane concentration. The E2 granular production was considerably lower than the one corresponding to the base case E1. An increase in the hydrogen flow rate, for the same initial PSDs (i.e., for identical minimum fluidization velocity), causes an increase in the flow of gas that circulates as bubbles. Higher gas flow rates lead to lower gas residence time, reducing the efficiency of capturing fines (Hsu et al., 1984a). This physical interpretation of the total flow rate effect is in good agreement with the observed experimental granular production and the calculated average scavenging factors. In fact $\alpha$ for E2, was about half of the corresponding value for E1.

For E3 the spout temperature was increased respect to the one of E1. High spout temperatures favor the homogeneous reaction and consequently the fines generation. Since granular production for E3 was almost equivalent to that of E1, the higher homogeneous reaction extension for E3 was balanced with higher scavenging efficiency than that corresponding to E1. In fact, the higher E3 fines generation in the spout zone allows for the powder higher probability of being captured as it travels through the fluidized bed (Rohatgi et al., 1982). To further study the effect of temperature, the fluidized bed temperature was also varied (E4). For the applied disturbance, the difference in silane conversion for experiments E1 and E4 was almost negligible. The E4 experimental results indicate a slight diminution in the granular production, behavior that can be explained in terms of the lower silane concentration, the lower gas temperature and the scavenging efficiency. Indeed, the fitted $\alpha$ for E4 was a little lower than that found for E1, probably due to the lower fines concentration and gas temperature. According to Lai et al. (1986) and Hsu et al. (1984b), the solid-solid interactions (collection efficiency of fines by large particle) are favored by temperature.

The inlet silane concentration was also varied; for E5 it was increased by 21% with respect to the base case (E1). The granular production and mean final particle diameter were higher than those corresponding to E1. It has been reported that increases in the silane concentration lead to more powder formation (Tilg and Mleczko, 2000; Hsu et al., 1984a). Consequently the scavenging phenomenon should be more important for the E5 operating conditions in order to fit the observed higher granular production, indeed the E5 $\alpha$ value was 27% higher than that of E1. As a result of the higher silane concentration, the particle growth rate for E5 increased about a 20%.

Regarding the agglomeration efficiencies, the kernel factors were of the same order of magnitude for experiments E1 to E4. For the studied operating conditions, only the silane inlet concentration had a noticeable effect on the aggregation. Although augments in the silane concentration favor agglomeration processes, the higher particle growth rate of experiment E5 reduces the number of smaller particles (which are the only ones that can undergo aggregation) and hence the probability of collision between them.

The previous analysis indicates that the scavenging factor seems to be mainly dependent on the total gas flow rate; the higher total gas flow rates (or lower gas residence time) the lower scavenging factors. This relationship is in good agreement with the results published by Hsu et al. (1984a). Besides, the scavenging efficiencies were also found to be dependent on the silane concentration. Higher silane concentration leads to both higher heterogeneous and homogeneous reaction rates (equations 2 and 3). All this leads to more fines being produced, higher fines density and as a result higher particle-fines interactions. It is indeed expected that, under these conditions, the higher fines concentrations with an increased probability of particles-fines collisions, lead to higher scavenging factors. For these reasons, the scavenging factors were correlated with the inlet silane concentrations that account for either hydrogen or silane gas flow rates. Figure 7 shows the scavenging factors for the experiments E1 to E5 as function of the silane concentration. As it can be seen, all the scavenging factors are correlated well via a linear regression. For modeling purposes, the proposed correlation may give an estimation of the scavenging factor that can be adopted in the absence of experimental data. Images of particles are in good agreement with the scavenging factors calculated for some experiments.

For all the experiments (E1 to E5) the adjusted CVD-SSBR model allows to well predict the dynamic evolution of bed mass and mean particle diameter and the particles size distribution over time. As an example of the goodness of the model for an experiment with high initial silane concentration (experiment E5), Figure 8 and 9 show the mean particle diameter as function of time and the PSD after six hours of operation, respectively.

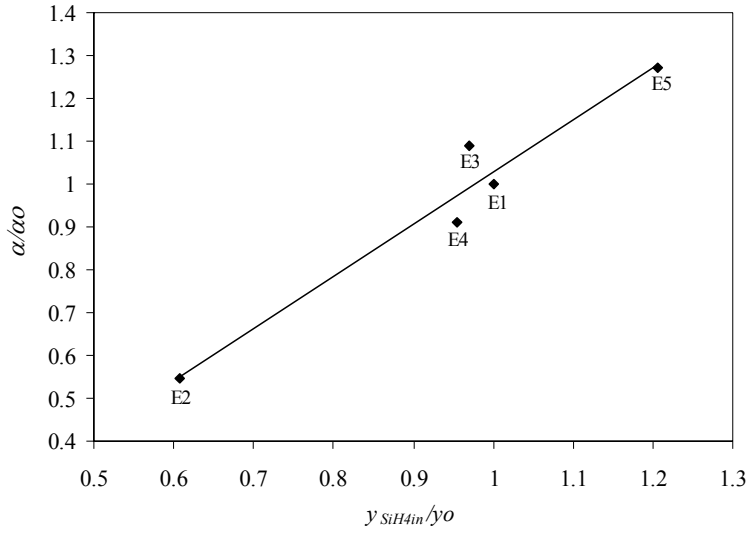


**Figure 7:** Scavenging factor as a function of the inlet silane concentration for experiments E1 to E5.

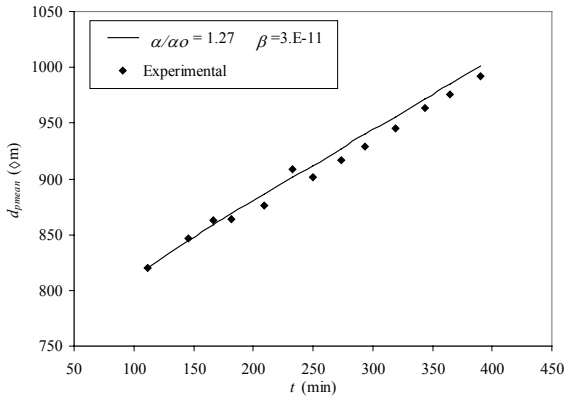


**Figure 8:** Experimental and predicted mean particle diameter as function of time for E5.

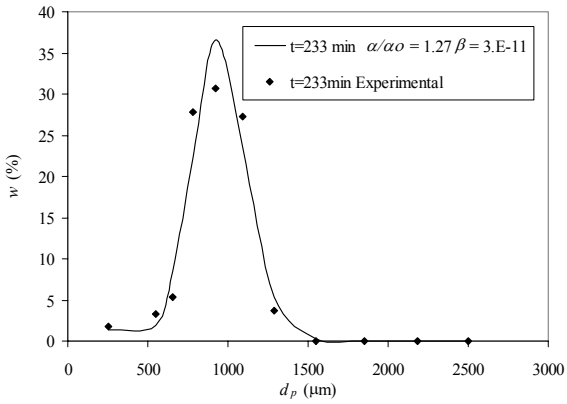


**Figure 9:** Experimental and predicted PSD at $t$ =233 min for E5.

The model was also tested for longer experimental runs (several days) with multiple seeds additions and sample extractions, aiming to gain understanding for the simulation of continuous operation. Figure 10 reports the experimental and calculated (based on the constant value of the base case $\alpha o$) dimensionless bed mass as function of time. The stepwise shape of the curves is related to the seeds additions and samples withdrawn that occur periodically. The bed mass is quite well predicted up to around 1500 min. After this time a slight overestimation is observed. It is important to note that the hydrogen flow was continuously increased to keep fluidizing a bed that was growing. To better fit the experimental data, $\alpha$ was corrected by the relationship between the instant silane concentration and the initial one (see black curve in Figure 10). This dynamic adjustment allowed an excellent prediction of the total bed mass for the run duration. The proposed equation for updating the scavenging factor is in good agreement with the dependence found for short-term batch operations.

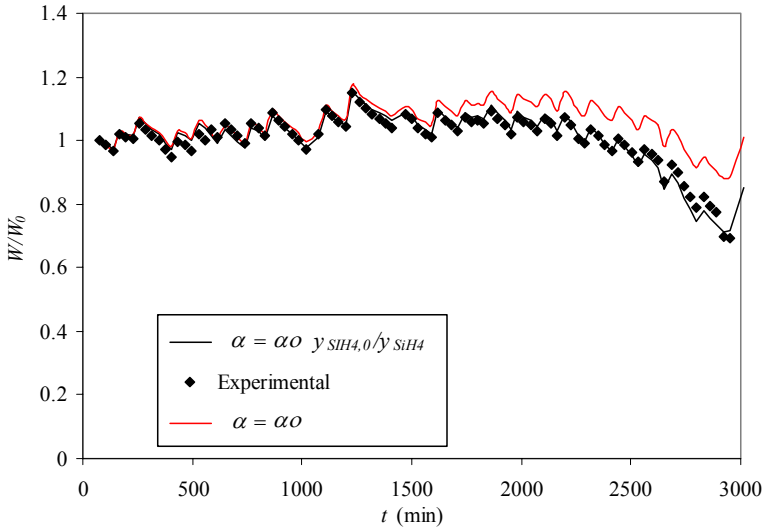


**Figure 10:** Experimental and predicted bed masses as function of time for a long experimental run with multiple seeds additions and sample extraction.

## 4. CONCLUSIONS

a) A comprehensive multiphase gas-solid mathematical model was implemented to describe the batch growth of silicon particles in a CVD submerged spouted bed reactor.
b) The proposed multiphase reactor representation is a phenomenological model that incorporates hydrodynamic, interphase mass exchange between the different fluidized bed regions (spout or grid zone, bubbles and emulsion phase) and applicable kinetic rates for both heterogeneous and homogeneous reactions.
c) The model includes an applicable population balance representing the growth and aggregation of silicon particles.
d) The simulation of the CVD system was successfully implemented via a numerical procedure that solves the submerged spouted bed reactor and the population balance equation compartments sequentially.
e) The proposed CVD multiphase reactor model, which involves two adjustable parameters (scavenging factor and agglomeration efficiency), was tested under an ample range of operating and dynamic conditions including particle additions and extractions. This model successfully simulates experimental data obtained from operation in a pilot scale reactor at REC Silicon Inc.
f) Based on experimental data obtained for pilot-scale runs with different operating conditions, the scavenging factor was successfully correlated as a function of the silane concentration. This correlation was found appropriate either for short- or long-term batch operations.

## ACKNOWLEDGEMENTS

We would like to express our appreciation to the REC Silicon Inc., the Universidad Nacional del Sur, the Consejo Nacional de Investigaciones Científicas y Técnicas (CONICET), and the Natural Sciences and Engineering Research Council of Canada (NSERC), organizations that financially supported the development of this research.

## NOTATION

$a_j$ Specific area of spout, $m_j^2/m_j^3$.
$A_{rj}$ Spout cross-sectional area, $m_j^2$.

$B_A$ Birth term for agglomeration, $\#_p$ /$m_p^3$s.
$C_D$ Drag coefficient.
$C_{H2}$ Hydrogen concentration, kmol/$m^3$.
$C_0$ Nozzle discharge coefficient.
$C_{SiH4}$ Silane concentration, kmol/$m^3$.
$D_A$ Death term for agglomeration, $\#_p$ /$m_p^3$s.
$d_b$ Bubble equivalent diameter, $m_b$.
$D_{hole}$ Nozzle outlet diameter, m.
$D_{mix}$ Molecular diffusion coefficient of the gas mixture, $m_g^2$/s.
$D_{pipe}$ Nozzle inlet diameter, m.
$D_R$ Reactor inner diameter, $m_r$.
$d_p$ Particle diameter, $m_p$.
$d_{p,mean}$ Mean particle diameter, $m_p$.
$F$ Molar flow rate of the gas mixture, kmol/s.
$Fo_{H2}$ Reference hydrogen molar flow rate, kmol/s.
$Fo_{SiH4}$ Reference silane molar flowrateflow rate, kmol/s.
$F_{mf}$ Molar flow rate of the gas mixture at minimum fluidization conditions, kmol/s.
$g$ Gravity acceleration, m/$s^2$.
$g_c$ Conversion factor, kg m/N$s^2$.
$G$ Particle growth rate [d$L$/d$t$], $m_p^3$/s.
$Go$ Reference particle growth rate, $m_p^3$/s.
$GP$ Granular production, %.
$GPo$ Reference granular production, %.
$H$ Total bed height, $m_r$.
$H_{mf}$ Bed height at minimum fluidization conditions, $m_r$.
$h_j$ Spout penetration, $m_j$.
$K_{bc}$ Interchange coefficient between bubble and clouds, $m_g^3$/$m_b^3$s.
$K_{be}$ Interchange coefficient between bubble and emulsion, $m_g^3$/$m_b^3$s.
$K_{ce}$ Interchange coefficient between clouds and emulsion, $m_g^3$/$m_b^3$s.
$k_{het}$ Kinetic constant of Iya et al. (1982), m/s.
$k_{hom}$ Kinetic constant of Hogness et al. (1936), 1/s.
$K_{H2}$ Kinetic constant of Furusawa et al. (1988), 1/kPa.
$k_j$ Mass transfer coefficient between spout and emulsion phase, kg/$m_j^2$s.
$K_{SiH4}$ Kinetic constant of Furusawa et al. (1988), 1/kPa.
$k_{so}$ Kinetic constant of Furusawa et al. (1988), m/s.
$K_v$ Kinetic constant of Furusawa et al. (1988), 1/kPa.
$k_{vo}$ Kinetic constant of Furusawa et al. (1988), 1/s.
$L$ Particle volume, $m_p^3$.
$M$ Number of classes on the size grid.
$M_{mix}$ Gas mixture molar weight, kg/kmol.
$M_{Si}$ Silicon molar weight, kg/kmol.
$M_{SiH4}$ Silane molar weight, kg/kmol.
$n$ Number density, $\#_p$ /$m_p^3$.
$N_{bubble}$ Total number of bubbles, $\#_b$.
$N$ Number of particles, $\#_p$.
$P$ Pressure, kPa.
$Q_{hole}$ Total volumetric flow rate through the nozzle, $m_g^3$/s.
$R$ Universal gas constant, kPa $m^3$/kmol K.
$r_{het}$ Heterogeneous reaction rate, kmol/$m_p^2$s.
$r_{hetem}$ Heterogeneous reaction rate in the emulsion, kmol/$m_p^2$s.
$r_{hetj}$ Heterogeneous reaction rate in the spout, kmol/$m_p^2$s.
$r_{hom}$ Homogeneous reaction rate, kmol/$m_g^3$s.
$r_{homb}$ Homogeneous reaction rate in the bubbles, kmol/$m_g^3$s.
$r_{homem}$ Homogeneous reaction rate in the emulsion, kmol/$m_g^3$s.
$r_{homj}$ Homogeneous reaction rate in the spout, kmol/$m_g^3$s.
$S_{pem}$ External surface of the particles in the emulsion, $m_p^2$.

$S_{pi}$ External surface of the particles in class i, $m_p^2$.
$S_{pj}$ External surface of the particles in the spout, $m_p^2$.
$S_{pt}$ Total external surface of the particles, $m_p^2$.
$t$ Operating time, s.
$t_R$ Bubble residence time $[(z-h_j)/U_b]$, s.
$T$ Gas temperature, K.
$T_b$ Fluidized bed temperature, K.
$T_j$ Spout temperature, K.
$To$ Reference gas temperature, K.
$U_b$ Velocity of the bubble, $m_r$/s.
$U_j$ Gas velocity in the spout, $m_g^3/m_r^2$s.
$U_{mf}$ Gas velocity at minimum fluidization conditions, $m_g^3/m_r^2$s.
$U_0$ Superficial gas velocity (based on empty tube), $m_g^3/m_r^2$s.
$V_b$ Volume per bubble, $m_b^3/\#_b$.
$V_{gem}$ Gas volume at the emulsion phase, $m_g^3$.
$v_{sa}$ Particle velocity in the annulus, m/s.
$v_{sj}$ Particle velocity in the spout, m/s.
$w$ Particle mass fraction.
$W$ Total particle mass, kg.
$Y$ Expansion factor.
$yo$ Reference $SiH_4$ molar fraction.
$y_{SiH4b}$ $SiH_4$ molar fraction in the bubbles.
$y_{SiH4em}$ $SiH_4$ molar fraction in the emulsion.
$y_{SiH4in}$ $SiH_4$ molar fraction at the reactor inlet.
$y_{SiH4j}$ $SiH_4$ molar fraction in the spout.
$y_{SiH4hj}$ $SiH_4$ molar fraction at the spout penetration.
$z$ Axial distance measured from the bottom of the bed, m.

***Subscripts***

*0* Initial.
*a* Annulus.
*b* Bubble.
*Bed* Fluidized bed.
*em* Emulsion.
*f* Final.
*g* Gas.
*i* At the $i^{th}$ size range.
*in* Inlet.
*j* Spout.
*p* Particle.
*r* Reactor.

***Superscripts***

* After sample removal.

***Greek Letters***

$\alpha$ Scavenging factor.
$\alpha o$ Reference scavenging factor.
$\beta_{ij}$ Agglomeration kernel or efficiency, $1/\#_p$s.
$\delta_{ij}$ Dirac-delta function.
$\varepsilon_a$ Void fraction in the annulus, $m_g^3/m_a^3$.
$\varepsilon_j$ Void fraction in the spout, $m_g^3/m_j^3$.

$\varepsilon_{mf}$ Void fraction at minimum fluidization conditions, $m_g^3/m_{em}^3$.
$\eta$ Defined by Equation (19).
$\Delta P_b$ Bed pressure drop, kPa.
$\Delta P_d$ Distributor pressure drop, kPa.
$\Delta t$ Computation time step, s.
$\lambda$ Ratio $D_{hole}/D_{pipe}$.
$\rho_g$ Gas molar density, $kmol/m_g^3$.
$\rho_p$ Particle density, $kg/m_p^3$.
$\phi_s$ Particle spherecity.

## REFERENCES

Alexopolous, A.H., Roussos, A.I., Kiparissides, C., "Part I: Dynamic Evolution of the Particle Size Distribution in Particulate Processes undergoing Combined Particle Growth and Aggregation", Chem. Eng. Sci., Vol. 59, No. 24, 5751-5769, (2005).

Basov, V. A., Markhevka, V. I., Melik-Akhnazarov, T. Kh., Orochko, D. I., "Investigation of the Structure of a Nonuniform Fluidized Bed, International Chemical Engineering, Vol. 9, 263-166, (1969).

Behie, L. A., Kehoe, P., "The Grid Region in a Fluidized Bed Reactor", AIChE J., Vol. 19, No. 5, 1070-1072, (1973).

Caussat, B., Hemati, M., Couderc, J.P., "Silicon Deposition from Silane or Disilane in a Fluidized Bed-Part I: Experimental Study", Chem. Eng. Sci., Vol. 50, No. 22, 3615-3624, (1995a).

Caussat, B., Hemati, M., Couderc, J.P., "Silicon Deposition from Silane or Disilane in a Fluidized Bed-Part II: Theoretical Analysis and Modeling", Chem. Eng. Sci., Vol. 50, No. 22, 3625-3635, (1995b).

Davidson, J. F., Harrison, D., "Fluidized Particles", Cambridge University Press, Cambridge, (1963).

Errazu A. F., de Lasa H. I., Sarti F., "A Fluidized Bed Catalytic Cracking Regenerator Model - Grid Effects", The Canadian Journal of Chemical Engineering, Vol. 57, 191-197, (1979).

Furusawa T., Kojima T., Hiroha H., "Chemical Vapor Deposition and Homogeneous Nucleation in Monosilane Pyrolysis within Interparticle Spaces - Application of Fines Formation Analysis to Fluidized-Bed CVD", Chemical Engineering Science, Vol. 43, No. 8, 2037-2042, (1988).

Grace, J.R., "Modeling and Simulation of Two-Phases Fluidized Bed Reactor", Chemical Reactor Design and Technology, Martinus Nijhoff Publishers, 245-289, (1986).

Haider, A., Levenspiel, O., "Drag Coefficient and Terminal Velocity of Spherical and Nonspherical Particles", Powder Technology, Vol. 58, 63-70, (1989).

Heinrich S., Peglow M., Ihlow M., Henneberg, M., Mörl L., "Analysis of the Start-up Process in Continuous Fluidized Bed Spray Granulation by Population Balance Modeling", Chem. Eng. Sci., Vol. 57, No. 20, 4369-4390, (2002).

Hogness, T. R., Wilson, T. L., Johnson, W. C., "Thermal Decomposition of Silane", Journal of the American Chemical Society, Vol. 58, 108-112, (1936).

Hsu, G., Rohatgi, N., Morrison, A., "Fines in Fluidized Bed Silane Pyrolysis", J. Electrochemical Society, Solid-State Science and Technology, Vol. 131, No. 3, 660-663, (1984a).

Hsu, G., Morrison, A., Rohatgi, N., Lutwack, R., MacConnnell, T., "Fluidized Bed Silicon Deposition", Conference Record of the IEEE, Photovoltaic Specialists Conference, 553-557, (1984b).

Hsu, G., Rohatgi, N., Houseman, J., "Silicon Particle Growth in a Fluidized-Bed Reactor", AICHE Journal, Vol. 33, No. 5, 784-791, (1987).

Iya, S. K., Flagella, R. N., DiPaolo, F. S., "Heterogeneous Decomposition of Silane in a Fixed Bed Reactor", Journal of the Electrochemical Society, Vol. 129, No. 7, 1531-1535, (1982).

Kato, K., Wen, Y.C., "Bubble Assemblage Model for Fluidized Bed Catalytic Reactors", Chem. Eng. Sci.,Vol. 24, No. 8, 1351-1369, (1969).

Kojima, T., Kimura, T., Matsukata, M., "Development of Numerical Model for Reactions in Fluidized Bed Grid Zone-Application to Chemical Vapor Deposition of Polycristalline Silicon by Monosilane Pyrolysis", Chem. Eng. Sci., Vol. 45, No. 8, 2527-2534, (1990).

Kumar S., Ramkrishna, D., "On the Solution of Population Balance Equations by Discretization-I. A Fixed Pivot Technique", Chem. Eng. Sci., Vol. 51, No. 8, 1311-1332, (1996).

Kumar S., Ramkrishna, D., "On the Solution of Population Balance Equations by Discretization-III. Nucleation, Growth and Aggregation of Particles", Chem. Eng. Sci., Vol. 52, No. 24, 4659-4679, (1997).

Kunii D., Levenspiel O., "Bubbling Bed Model. Model for Flow of Gas through a Fluidized Bed", Ind. Eng. Chem. Fundam., Vol. 7, No. 3, 446-452, (1968).

Kunii D., Levenspiel O., Fluidized Reactor Models. 1. For Bubbling Bed of Fines, Intermediate and Large Particles. 2. For the Lean Phase: Freeboard and Fast Fluidization", Ind. Eng. Chem. Res., Vol. 29, No. 7, 1226-1234, (1990).

Kunii D., Levenspiel O., "Fluidization Engineering", J. Wiley and Sons, New York, (1991).

Lai, S., Dudukovic, M.P., Ramachandran, P.A., "Chemical Vapor Deposition and Homogeneous Nucleation on Fluidized Bed Reactors: Silicon from Silane", Chem. Eng. Sci., Vol. 41, No. 4, 633-641, (1986).

Lee, G., Yoon, E.S., Lim, Y.-I., Le Lann, J.M., Meyer, X.-M., Joulia, X., "Adaptive Mesh Method for the Simulation of Crystallization Processes Including Agglomeration and Breakage: the Potassium Sulfate System", Ind. Eng. Chem. Res., Vol. 40, 6228-6235, (2001).

Li, K.Y., Peng, S.H., Ho, T.C., "Prediction of Silicon Powder Elutriation in a Fluidized-Bed Reactor for the Silane Decomposition Reaction", Fluidization and Fluid-Particle Systems-Fundamentals and Applications, AIChE Symposium Series, Vol. 85, No. 270, 77-80, (1989).

Lord, S.M., Milligan, R. J., "Advanced Silicon Materials", US Patent, 5, 798, 137, (1998).

Miller, R.W., "Flow Measurement Engineering Handbook", New York, Mc Graw Hill, (1996).

Ramkrishna, D., "Population Balances", Academic Press, London, (2000).

Rohatgi, N.K., Hsu, G.C., Lutwack, R., "Silane Pyrolysis in a Fluidized Bed Reactor", Proceedings The Electrochemical Society, 82-8, 477-487, (1982).

Sarti D., Einhaus R., "Silicon Feedstock for the Multi-crystalline Photovoltaic Industry", Solar Energy Materials and Solar Cells, Vol.72, 27-40, (2002).

Tejero-Ezpeleta, M.P., Buchholz, S., Mleczko, L., "Optimization of Reaction Conditions in a Fluidized-Bed for Silane Pyrolysis", The Canadian Journal of Chemical Engineering, Vol. 82, 520-528, (2004).

Tilg, A., Mleczko, L., "Predictive Model of Silane Pyrolysis in a fluid-bed reactor", Silicon for the Chemical Industry V, Tromsø, Norway, (2000).

Woditsch P., Koch W., "Solar Grade Silicon Feedstock Supply for the PV Industry", Solar Energy Materials and Solar Cells, Vol.72, 11-26, (2002).